Turbulent trailing edge noise estimation using a RANS-based statistical noise model

C.A. Albarracin, C.J. Doolan, C.H. Hansen and L.A. Brooks

School of Mechanical Engineering, The University of Adelaide, Adelaide, South Australia

ABSTRACT

The prediction capability of a RANS-based Statistical Noise Model (RSNM) is assessed by applying it to a sharp-edged symmetric flat strut at a Reynolds number of Re = 500,000 and zero angle of attack. The method uses a rigid-half-plane Green's function to calculate the far-field spectra generated by the turbulence in the vicinity of the trailing edge. Because the exact form of the turbulent sources is in general not available, a model of the turbulent velocity cross-spectrum must be assumed. The cross-spectrum model must accurately reflect the frequency and phase distribution in the boundary layer close to the trailing edge, but is otherwise arbitrary. The model used in this study is Gaussian, containing velocity, time and length scales that are defined in terms of the turbulence statistics obtained from a steady RANS solution. The predicted sound spectrum shows the correct slope and levels for frequencies ranging from 300 Hz to 2 kHz.

INTRODUCTION

Trailing edge (TE) noise is an issue in many engineering applications such as fixed and rotary wing aircraft, fans, wind turbines and submarines. Efficient prediction methods for trailing edge noise are essential for enabling the design of silent airfoils for these applications.

Trailing edge noise occurs when flow unsteadiness (turbulence) in the boundary layer over an airfoil interacts with the trailing edge. The edge acts as an abrupt change in acoustic impedance, scattering the sound waves produced by the turbulence and enhancing the sound radiation to the far field. The edge effectively destroys some of the cancelations that would normally occur between the individual monopole components of the quadrupole sources (turbulent eddies) if the edge were not present, transforming the near field pressure fluctuations into propagating acoustic waves. A detailed explanation of the trailing edge noise mechanism can be found in Goldstein (1976, pp. 174-181).

There are three main methods generally used for calculating TE noise; semi-empirical methods, direct methods and hybrid methods.

Semi-empirical methods relate the far field noise to boundary layer properties such as boundary layer thickness or displacement thickness. The most widely used is the Brooks, Pope and Marcolini (BPM) method, which provides an expression for the far field noise in 1/3 octave bands, based on a spectral shape function that depends on the Strouhal number and a scaling based on boundary layer displacement thickness. While efficient and accurate, the range of application of semi-empirical methods is limited, and they cannot take into account the effect of trailing edge modifications such as serrations.

Direct methods calculate the fluid dynamics and acoustics in a single step. They do so by solving the compressible Navier Stokes equations using either direct numerical simulation (DNS) or large eddy simulation (LES). This approach has been successfully used by several researchers (Marsden et al., 2008; Jones and Sandberg 2009; LeGarrec et al., 2008), but the computational demands of DNS and LES are too large for this approach to be practical for airfoil design applications.

Hybrid methods de-couple the flow calculation from the sound calculation, as the latter can be done as a post processing step. This separation of the sound generation and propagation processes makes the hybrid approach more efficient, as a fine mesh is only required in the region close to the airfoil, where viscous effects are important. The sound sources are generally obtained from LES or DNS and the far field noise can be calculated by means of an acoustic analogy. This approach has been shown to be as accurate as the direct approach (Khalighi et al., 2010) at a fraction of the computational cost. Recent examples of TE noise calculations using this approach include Christophe et al., (2009) and Winkler et al., (2009).

While more computationally efficient than direct methods, hybrid methods based on LES or DNS calculations are still too computationally demanding to be of practical use in airfoil design. Due to its more modest computational requirements, the solution of the steady Reynolds Averaged Navier Stokes (RANS) equations presents itself as a more practical approach to obtain the required flow data to perform TE noise calculations. However, sound generation is inherently time dependent, so the time averaged information available from a RANS solution is not sufficient by itself to perform noise calculations. To cope with this limitation, different approaches based on statistical data provided using RANS equations have been developed; namely stochastic noise generation and radiation (SNGR) and statistical modelling of the turbulent sources.

The SNGR approach generates a synthetic turbulent source field in the time domain, based on prescribed statistical information of the flow, which can be obtained from a RANS solution. It has been succesfully applied to TE noise calculations (Ewert 2008; Ewert et al., 2009), and has also been used successfully for a variety of aerodynamic noise problems, such as landing gear noise (Dobrzynski et al., 2008), and jet and cavity noise (Mesbah 2006). The drawback of this approach is that the computational requirements to generate and

store the turbulence time data, and to calculate the far field noise, are of the same order or larger than the RANS calculations that provide the statistics to generate the turbulent sources.

Most other RANS based methods for TE noise modelling rely on an estimation of the surface pressure spectrum, which is then converted to a far field acoustic spectrum using a diffraction analogy technique (Chandiramani 1974). Recent examples of TE noise calculations using this approach include the work of Kamruzzaman et al., (2007, 2008) and Glegg et al., (2010).

A limitation of surface pressure models is the assumption of homogeneous turbulence in the spanwise and streamwise directions, a condition that is unlikely to hold in many trailing edge configurations, particularly when serrations or other spanwise modifications are used.

A RANS-based statistical noise model (RSNM) has been proposed by Doolan et al., (2010), that does not require the assumption of homogeneous turbulence. This method uses a semi-infinite hard-plane Green's function to calculate the acoustic far field directly, using a statistical model of the turbulent sources in the boundary layer in the vicinity of the trailing edge. The method requires a model of the turbulent velocity cross-spectrum, which must accurately represent the frequency and phase distribution in the boundary layer. This approach is based on the work of Tam and Auriault (1999) and Morris and Farassat (2002), who developed a similar model for jet noise applications.

In this paper, the prediction capability RSNM is assessed by applying it to a sharp-edged symmetric flat strut at a Reynolds number based onchord of Re = 500,000 at zero angle of attack.

NOISE PREDICTION METHOD

The acoustic spectrum $S(\boldsymbol{x},\omega)$ at a point $\boldsymbol{x}$ in the far field as a function of frequency is given by

$$S(\mathbf{x},\omega) = \sum_{V(\mathbf{y}_1)}\sum_{V(\mathbf{y}_2)} \left\{\gamma\left[u_r'^{*}(\mathbf{y}_1)\hat{u}_r'^{*}(\mathbf{y}_2)\right] F(\mathbf{y}_1)F(\mathbf{y}_2)\right\} dV(\mathbf{y}_1)dV(\mathbf{y}_2) \tag{1}$$

where

$$\gamma = \frac{\rho_0^2 \omega \sin\phi \cos^2\left(\frac{\theta}{2}\right)}{8\pi^3 c r_0(\mathbf{y}_1)^{3/2} r_0(\mathbf{y}_2)^{3/2} R(\mathbf{y}_1)R(\mathbf{y}_2)} \tag{2}$$

and

$$\sin\phi = \frac{r}{\sqrt{r^2 + \left(z - z_0\right)^2}} \tag{3}$$

where ω is the angular frequency, θ is the angle between the observer and the chord plane with the origin located at the trailing edge plane (see figure 1), c is the speed of sound, R is the distance between the observer and the fluid element, r_0 is the distance from the edge to the fluid element, V is the volume of fluid considered in the noise summation, $\mathbf{y}$ is the vector location of the fluid element (source) and the subscripts 1 and 2 refer to the fluid elements used in each summation step.

In this article, the following notation is used: u^* is the Fourier transform of u, $\hat{u}$ is the complex conjugate of u.

F is a mean flow function defined by

$$F(\mathbf{y}) = \left\{\left(\bar{U}_r - f_a\bar{U}_\theta\right)\cos\left(\frac{\theta_0}{2}\right) - \left(\bar{U}_r + f_a\bar{U}_\theta\right)\sin\left(\frac{\theta_0}{2}\right)\right\} \tag{4}$$

Where θ_0 is the angle between a turbulent source and the trailing edge plane, $\bar{U}$ is the time averaged component of velocity and u' is the fluctuating component of velocity ($u = \bar{U} + u'$) and the subscripts r and θ ndicate radial and tangential components respectively. The quantity f_a is an anisotropy factor. For isotropic turbulence, $f_a = 1$.

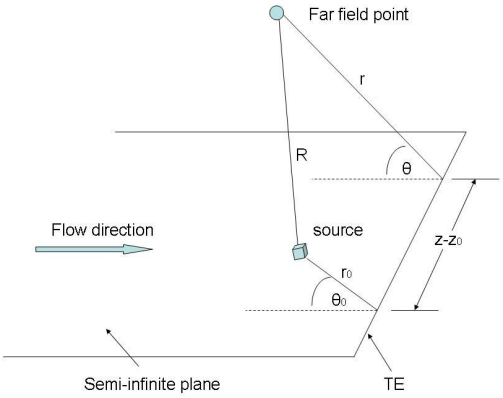

Figure 1. The Coordinate system used in the definition of equations 1, 2, 3 and 4.

With the exception of the velocity cross spectrum (the term in square brackets in Equation 1), all elements in equation 1 can be calculated directly from the RANS solution. In order to perform a noise calculation, a model for the velocity cross spectrum is required,

$$u_r'^{*}(\mathbf{y}_1)\hat{u}_r'^{*}(\mathbf{y}_2) = \Phi(\mathbf{y}_1.\mathbf{y}_2,\omega) \tag{5}$$

Cross spectrum model

The cross spectrum model used in this paper is given by

$$\Phi(\mathbf{y}_1,\xi,\omega) = \frac{A\sqrt{\pi}}{\omega_s}u_s^2 \exp\left(\frac{|\boldsymbol{\xi}|^2}{\ell_s^2} - \frac{\omega^2\left(1-M_c\right)^2}{4\omega_s^2}\right) \tag{6}$$

where M_c is the convection Mach number and A is an empirical constant that determines the strength of the correlation. The remaining variables are defined as

$$\boldsymbol{\xi} = \boldsymbol{\eta} - M_c c(\mathbf{i_r}\cos\theta_0 + \mathbf{i_\theta}\sin\theta_0)\tau, \quad \boldsymbol{\eta} = \mathbf{y_2} - \mathbf{y_1}, \tag{7}$$

and the turbulent scales are defined by

$$u_s = \sqrt{2k/3}, \qquad \omega_s = 2\pi/\tau_s, \qquad \tau_s = c_\tau k/\varepsilon, \qquad \ell_s = c_\ell k^{3/2}/\varepsilon. \tag{8}$$

where k (turbulent kinetic energy) and ε (dissipation rate of turbulent kinetic energy) are obtained from a RANS simulation and c_τ, c_ℓ and A are empirical constants determined by best fit to data. The constants c_τ and c_ℓ affect the time and length scales of the turbulence, respectively. This has the effect of modifying the frequency content of the resulting noise spectrum.

RANS SIMULATIONS

The mean flow data required for the calculation of the turbulent scales (k and ε) is obtained by means of a steady state RANS simulation, using the semi-implicit method for pressure-linked equations (SIMPLE) algorithm (Ferziger and Peric 1999), with a tolerance level set to 10^{-6}. Closure for the RANS equations was provided by the *k-ω SST* turbulence model (Menter 1992). The OpenFOAM (Weller et al., 1998) software package was used for all flow calculations.

Test case: symmetric strut

The test case studied was a 200 *mm* chord symmetric strut of 5 *mm* thickness, with a circular leading edge and a sharp trailing edge with a 12 degree apex angle and a span of 450 mm. In this study, two dimensional RANS simuations were performed, so the span of the airfoil was taken into account by means of an empirical spanwise correlation length in the noise calculations (Corcos 1964). The Reynolds number was set at Re_c = 500,000. A free stream turbulence intensity of 1.6 % was set for the simulations. The observer position was set at 0.585 *m* directly above the trailing edge. Moreau et al. (2011) provides the reference experimental data for this paper. A diagram of the strut is shown in Figure 2.

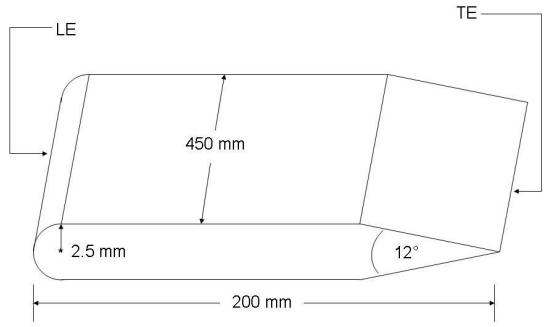

Figure 2. Diagram of symmetric strut.

Grid refinement study

The grid used for this study is shown in Figure 3. It was composed of four structured blocks and the necessary grid spacing was determined by comparing the results from a series of meshes that were successively refined. The initial mesh had a resolution of 117000 cells, which was increased by doubling the number of cells in both x and y directions for each refinement step. The resolution was increased until no change was observed in the mean velocity and turbulence intensity profiles at the near wake (0.6 *mm* from the TE). The mean velocity and turbulence intensity profiles are plotted against the experimental data from Moreau et al. (2011) in Figures 4 and 5 respectively. It is clear that there is no change in the results between the second and third refinement steps. Therefore, a resolution of 426000 cells was deemed sufficient to provide a grid independent solution. The RANS model calculates the velocity profile very well for most of the boundary layer, but underpredicts the velocity for $y^+ < 30$. It does not perform so well in predicting the turbulence intensity, where it is unable to resolve two distinct features of the experimentally measured profile; namely the peak at $y^+ = 60$ and the broad hump located in the region $400 < y^+ < 700$. This may be caused by the assumption of isotropic turbulence inherent in the *k-ω SST* turbulence model. It is expected that the use of a more complex anisotropic turbulence model like the Reynolds Stress Model (RSM) will provide better results in the calculation of the turbulence intensity profiles. This possibility will be investigated in future work. Contour plots of the turbulence intensity and mean velocity in the region near the trailing edge are shown in Figures 6 and 7, respectively.

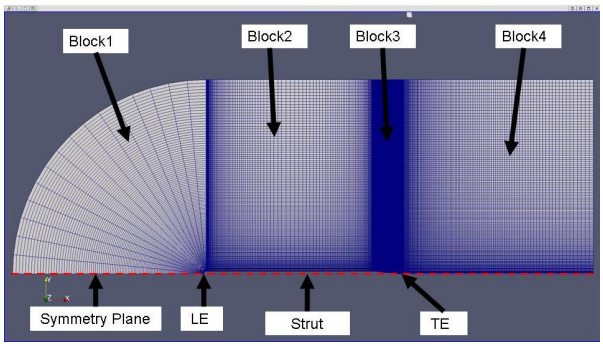

Figure 3. Mesh used for the RANS calculations. Flow direction from left to right.

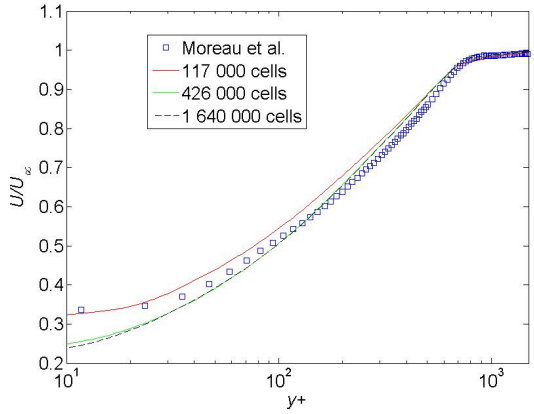

Figure 4. Mean velocity profiles calculated using the *k-ω SST* model and three mesh resolutions compared to experimental hot wire measurements at 0.003 chords downstream from the trailing edge.

ACOUSTIC RESULTS

Acoustic grid refinement

Once the flow data were obtained from a RANS calculation, the data were sampled onto an acoustic grid in order to perform the noise calculations. This grid extended over the boundary layer thickness δ in both wall normal and upstream directions, as shown in Figure 8. A grid refinement study was conducted in order to determine a grid independent solution. The results are shown in Figure 9. A resolution of 50 × 50 was deemed sufficient, since a further increase in resolution had no apparent effect on the predicted sound levels

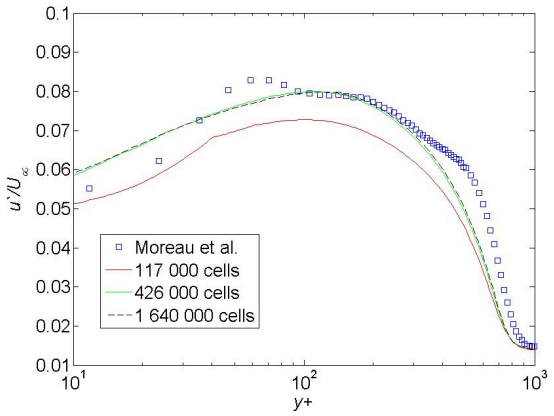

Figure 5. Turbulent intensity profiles calculated using the *k-ω SST* model for three mesh resolutions compared to experimental hot wire measurements at 0.003 chords downstream from the trailing edge.

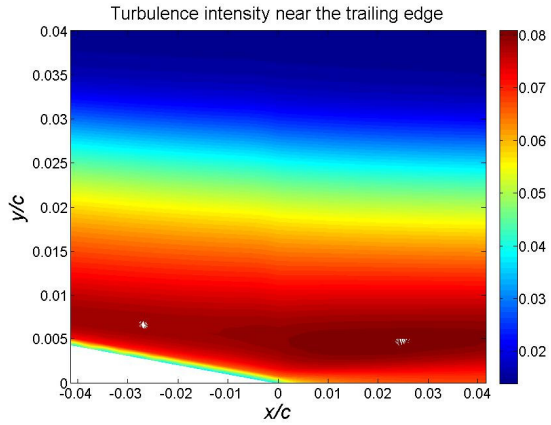

Figure 6. Turbulence intensity contours near the trailing edge. The region in white is part of the inner volume of the airfoil. The trailing edge is located at $y/c = x/c = 0$.

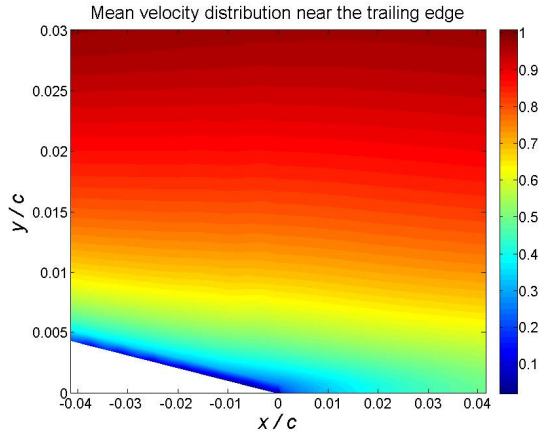

Figure 7. Mean velocity contours near the trailing edge. The region in white is part of the inner volume of the airfoil.The trailing edge is located at $y/c = x/c = 0$.

Comparison with experimental results

The spectral density calculated with RSNM is plotted against the experimental data obtained in the anechoic wind tunnel at the University of Adelaide (Moreau et al., 2011) in Figure 10. The values used for the empirical constants are $A = 10$, $c_\ell = 1$ and $c_\tau = 10.5$. The model predicts the correct slope and levels for frequencies between 300 and 2000 Hz, but the frequency roll off is too steep and severely under-predicts the sound levels for higher frequencies. The spectral hump in the experimental data close to 1.5 kHz corresponds to the interaction of the sound radiated from the trailing edge and two extension plates, placed at the contraction outlet of the wind tunnel in order to extend the potential core region (Moreau et al., 2011). It is therefore not surprising that the model is not able to predict this feature of the noise spectrum.

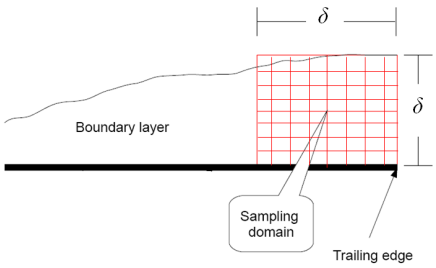

Figure 8. Diagram of the grid used for the acoustic calculations. The symbol δ represents the boundary layer thickness at the trailing edge.

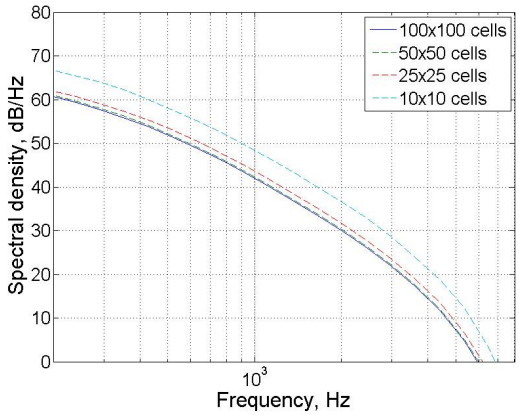

Figure 9. Spectral density at the observer position calculated using RSNM with four different acoustic grid resolutions.

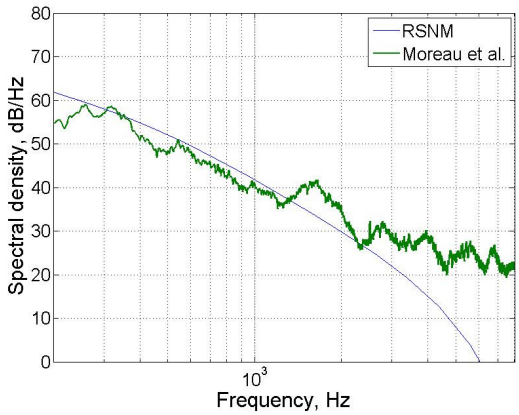

Figure 10. Spectral density in the far field calculated using a RSNM simulation, plotted against experimental data of Moreau et al., (2011).

CONCLUSIONS

The RSNM method has been applied to a symmetric flat strut at zero angle of attack and a Reynolds number of

Re=500,000. The predicted spectrum shows the correct slope and levels for frequencies between 300 Hz and 2 kHz, but the prediction deteriorates significantly for higher frequencies. The under prediction of the radiated sound at higher frequencies is most likely due to a poor prediction of the turbulent kinetic energy by the RANS model, which is used to calculate the turbulent scales in the cross spectrum model. It is also possible that the form of the cross spectrum model used in this work is not the most appropriate for boundary layer flows, since it is based on a two-point velocity correlation model derived for jets. This will be investigated in future work. The values chosen in this paper for the empirical constants A, c_τ and c_ℓ might not be suited for all of flow conditions, and a study of their range of application will be conducted in the future, when RSNM is applied to other airfoil shapes.

REFERENCES

Brooks, T. F., Pope, D. S. & Marcolini, M. A. (1989), '*Airfoil self-noise and prediction*', NASA Reference publication, 1218.

Chandiramani, K. L. (1974), 'Diffraction of evanescent waves, with applications to aerodynamically scattered sound and radiation from unbaffled plates', *Journal of the Acoustical. Society of America,* 55, 19-29

Christophe, J., Anthoine, J. & Moreau, S. (2009), 'Trailing edge noise of a controlled-diffusion airfoil at moderate and high angle of attack', *Proceedings of the 30th AIAA Aeroacoustics Conference*. Miami, Florida, 11-13 May.

Corcos, G. M. (1964), 'The structure of the turbulent pressure field in boundary layer flows', *Journal of Fluid Mechanics* 18, 353-378.

Dobrzynski, W., Ewert, R., Pott-Pollenske, M., Herr, M. & Delfs, J. (2008), 'Research at DLR towards airframe noise prediction and reduction', *Aerospace Science and Technology*, 12, 80–90.

Doolan, C., Albarracin, C., Hansen, C. (2010), 'Statistical estimation of turbulent trailing edge noise', *Proceedings of the 20th International Congress on Acoustics, ICA 2010*, Sydney, Australia, 23–27 August.

Ewert, R. (2008), 'Broadband slat noise prediction based on CAA and stochastic sound sources from a fast random particle-mesh (RPM) method' *Computers & Fluids*, 37, 369–387.

Ewert, R. & Al, E. (2009), 'RANS/CAA based prediction of NACA 0012 broadband trailing edge noise and experimental validation', *Proceedings of the 15th AIAA/CEAS Aeroacoustics Conference.* Miami, Florida. 11-13 May.

Ferziger, J., & Peric, M. 1999, *Computational methods for fluid dynamics*. Springer Berlin.

Glegg, S., Morin, B., Atassi, O. & Reba, R. (2010), 'Using Reynolds-Averaged Navier–Stokes Calculations to Predict Trailing-Edge Noise' *AIAA JOURNAL*, 48.

Goldstein, M. *Aeroacoustics*. McGraw Hill, New York, 1976.

Jones, L. & Sandberg, R. (2009), 'Direct numerical simulations of noise generated by the flow over an airfoil with trailing edge serrations', *Proceedings of the 15th AIAA/CEAS Aeroacoustics Conference (30th AIAA Aeroacoustics Conference).* Miami, Florida. 11-13 May, 2009.

Kamruzzaman, M., Lutz, T., Herrig, A. & Kramer, E. (2008), 'RANS based prediction of airfoil trailing edge far-field noise: impact of isotropic & anisotropic turbulence', *Proceedings of the 14th AIAA/CEAS Aeroacoustics Conference (29th AIAA Aeroacoustics Conference).* Vancouver, British Columbia Canada. 5-7 May.

Kamruzzaman, M., Lutz, T. & Kramer, E. (2007), 'An approach to RANS based prediction of airfoil trailing edge far-field noise', *Proceedings of the Second International Meeting on Wind Turbine Noise.* Lyon France. 20-21 September.

Khalighi, Y., Mani, A., Ham, F. & Moin, P. (2010), 'Prediction of sound generated by complex flows at low Mach numbers' *AIAA JOURNAL,* 48.

Le Garrec, T., Gloerfelt, X. & Corre, C. (2008), 'Direct noise computation of trailing edge noise at high Reynolds numbers', *Proceedings of the 14th AIAA/CEAS Aeroacoustics Conference (29th AIAA Aeroacoustics Conference).* Vancouver, British Columbia Canada. 5-7 May.

Marsden, O., Bogey, C. & Bailly, C. (2008), 'Direct Noise computation of the turbulent flow around a zero-incidence airfoil' *AIAA JOURNAL*, 46.

Menter, F. (1992), *Improved two-equation k−w turbulence models for aerodynamic flows,* NASA Technical Memorandum. NASA Ames, CA.

Mesbah, M. 2006 'Flow noise prediction using the stochastic noise generation and radiation approach', PhD Thesis, Katholieke Universiteit Leuven, Belgium, 2006.

Moreau, D., Brooks, L. & Doolan, C. (2011), 'Experimental investigation of broadband trailing edge noise from sharp-edged struts', *Proceedings of the 17th AIAA/CEAS Aeroacoustics Conference*. Portland Oregon. 5-8 Jun.

Morris, P. & Farassat, F. (2002), 'Acoustic analogy and alternative theories for jet noise prediction', *AIAA JOURNAL*, 40.

Tam, C. & Auriault, L. (1999), 'Jet mixing noise from fine-scale turbulence'. *AIAA JOURNAL*, 37.

Weller, H., Tabor, G., Jasak, H. & Fureby, C. (1998), 'A tensorial approach to CFD using object orientated techniques', *Computers in Physics, 12(6):620–631.*

Winkler, J., Moreau, S. & Carolus, T. (2009), 'Large-eddy simulation and trailing-edge noise prediction of an airfoil with boundary-layer tripping', *Proceedings of the 30th AIAA Aeroacoustics Conference.* Miami, Florida. 11-13 May.